DOI: 10.1002/ejic.200800110

From Single-Molecule Precursors to Coupled Ag_2S/TiO_2 Nanocomposites

Márcia C. Neves,[a] Olinda C. Monteiro,[b] Rolf Hempelmann,[c] Artur M. S. Silva,[d] and Tito Trindade*[a]

Keywords: Nanostructures / Molecular precursors / Metal sulfides / Semiconductors

A single-source approach using mild temperatures was applied to prepare morphological well-defined and coupled TiO_2/metal–sulfide nanocomposites. Metal *N*-alkyldithiocarbamates were used as the precursors to the metal–sulfide nanophases and, in particular, Ag_2S nanostructures were investigated in more detail. These were observed as nanoislands at the surface of TiO_2 (anatase) particles, which were used as substrates. To explain the formation of these nanocomposite particulates, a tentative mechanism has been proposed which involves the controlled release of sulfide ions from an intermediate coordination compound. Because the growth of the metal sulfide can be controlled at the surface of a photoactive substrate, we anticipate the potential of this synthetic method to chemical design reasonable amounts of semiconductor-sensitized TiO_2, such as Ag_2S/TiO_2 nanocomposites.

Introduction

In recent years, the rational design of functional materials using moderate reaction conditions has been a general trend in materials chemistry.[1] In fact, this corresponds to a new paradigm in materials science in which, depending on the applications of the materials, their final properties can be tailored from the synthesis. In this sense, controlling the morphology of particulates appears to be obvious requirement to control size-dependent functionalities. A clear example of this trend is the high degree of control over the optical properties of semiconductor nanocrystals whose unique size-dependent behaviour can be tuned during the synthesis. Applications which rely on the size tunability of semiconductor nanocrystals have already been developed, such as in photoluminescent biotags and electroluminescence devices.[1]

Another important application envisaged for semiconducting nanoparticles is their use in photocatalytic processes with relevance for environmental decontamination.[2] The most investigated systems rely on TiO_2 photocatalysts, that can be coupled to a visible sensitizer which may be a metal complex, a dye or a second semiconducting nanophase.[3] Although less investigated, the use of nanosized particles as sensitizers shows advantages such as bandgap tuning for efficient light absorption and the ability for surface modification to avoid photocorrosion processes. For example, semiconductor nanocrystals absorbing in the visible region of the spectrum can promote the photocatalytic efficiency of TiO_2 photocatalysts by allowing efficient solar radiation harvesting. While considerable progress has been made in coupling nanoparticles of metal chalcogenides and metals with silica shells,[4] comparatively less has been done in coupling two semiconducting nanophases.[5] Examples of contributions in this field include the preparation of TiO_2-based nanocomposites containing either CdSe, Se, CdS, Bi_2S_3, Ag_2S, Ge or In_2O_3.[6] For the preparation of such nanocomposites, a range of colloidal methods have been used, but there is still a lack of synthetic strategies to produce reasonable quantities of pure nanocomposites which allow, simultaneously, the design of their final morphological characteristics. This led us to undertake the research reported here, in which TiO_2 submicrometric particles were mainly used as substrates because of their relevance in photocatalytic applications.

The use of single-molecule precursors to grow semiconducting thin films is well established.[7] In the last decade, this approach has also been investigated to synthesize a wide range of semiconductor nanocrystals.[8] In general, these methods involve the thermal decomposition of single-molecule precursors in a hot coordinating solvent.[8] More recently, we have shown that single-molecule precursors such as cadmium/zinc dithio- or selenocarbamates can also be used to modify the surface of silica particles with the respective metal chalcogenide.[9] The possibility of growing islands of a semiconducting nanophase of varying morpho-

[a] Department of Chemistry, CICECO, University of Aveiro, 3810-193 Aveiro, Portugal
Fax: +351-234-370-084
E-mail: tito@ua.pt
[b] Department of Chemistry and Biochemistry, CCMM, University of Lisbon,
Campo Grande, Ed. C8, 1749-016 Lisboa, Portugal
[c] Physical Chemistry, Saarland University,
66123 Saarbrücken, Germany
[d] Department of Chemistry, QOPNA, University of Aveiro, 3810-193 Aveiro, Portugal
Supporting information for this article is available on the WWW under http://www.eurjic.org or from the author.

logies at the silica surfaces is a striking feature of this method. The resulting coupled particles seem especially interesting for exploiting the synergy between the surface reactivity of the substrate, associated with the unique optical properties of the deposited semiconductor nanocrystals. It will be shown here that this approach gives us a convenient method to produce large amounts of several coupled metal chalcogenide/TiO_2. In this work the focus is on TiO_2/Ag_2S nanocomposites. Moreover, a tentative mechanism that can explain the formation of metal–sulfide phases using such an approach will be discussed here for the first time.

Results and Discussion

Metal–dithiocarbamate complexes in the presence of aliphatic amines yield the respective metal sulfide when subjected to moderate heating. In the presence of inorganic substrates, such as TiO_2 or SiO_2 particles, the metal–sulfide phase grows at the particles' surfaces.[9] As will be discussed later, this probably involves an intermediate metal complex[10] which then decomposes into metal sulfide. In the current work, this method was investigated to grow Ag_2S nanophases at the surface of synthetic TiO_2 (anatase) submicrometric particles. These TiO_2 particles were prepared by the hydrolysis of titanium(IV) ethoxide in ethanol followed by a calcination step to obtain TiO_2 particles. The average diameter of the particles was varied within the size range 100–600 nm by adjusting the chemical composition of the reaction mixture (see Experimental Section). Although rutile is the thermodynamically stable crystalline phase for TiO_2, anatase is very common at room temperature in fine divided powders, such as in pigments. Figure 1 contains representative SEM images showing the morphology of Ag_2S/TiO_2 nanocomposites. For comparison, a SEM image of the original TiO_2 particles is also shown.

The TiO_2 powders were dispersed in acetone without being submitted to any type of chemical surface modification. Figure 1 shows that in these conditions the TiO_2 surfaces become covered with a polycrystalline material which we assign to Ag_2S, as expected from the degradation of the metal *N*-alkyldithiocarbamate used. Thus, Figure 2 shows that this nanocomposite contains TiO_2 (*anatase*) and α-Ag_2S (*acanthite*) as the predominant crystalline phases. Moreover, these nanocomposite particles were further analysed by EDX which showed the expected peaks for Ag and S, as well as the peak of Ti due to TiO_2. For the several samples analysed, there was no observation of strong and single S peaks that could be assigned to elemental sulfur. This was also confirmed by XPS analysis of the nanocomposites, which showed only one S environment as a single doublet corresponding to S 2p3/2 and S 2p1/2 of sulfide species (see Supporting Information).[11]

The visible reflectance spectra of the nanocomposites recorded at different reaction times show an optical redshift in the absorption edge as the reaction proceeds, which is consistent with a growing process for nanocrystalline semiconductors.[9] This trend is illustrated in Figure 3a for the TiO_2/Ag_2S nanocomposite. For silica-supported semiconductors (e.g., SiO_2/CdS), a blueshift of the typical bandgap energy was also interpreted in terms of an electronic semiconductor-support interaction (SEMSI).[12] Despite some similarities of the systems reported here and those reported in the literature,[12] in the latter, the semiconductor nanophases were precipitated directly by adding sulfide to Cd^{II}-loaded SiO_2 particles. Hence, composites with distinct morphological characteristics and also with bigger average diameters were obtained compared with the nanomaterials reported here. Moreover, we observed blueshifts of the bandgap energy of nanocrystalline semiconductors (e.g., CdS and CdSe) deposited on substrates quite distinct from SiO_2 or TiO_2, such as reticulated polystyrene beads.

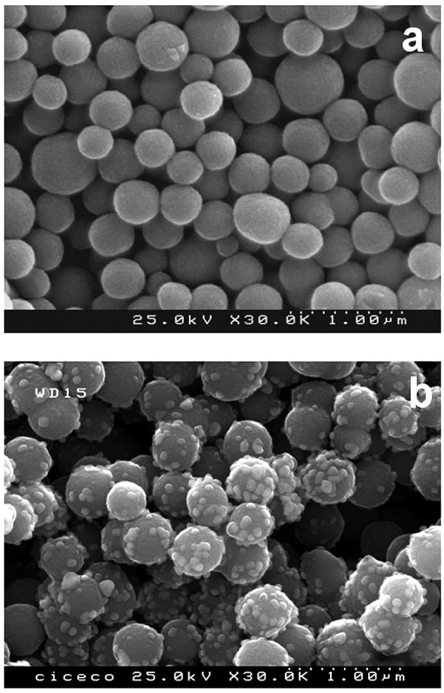

Figure 1. SEM images of TiO_2 (a) and TiO_2/Ag_2S (b) nanocomposites obtained for a reaction time of 8 h.

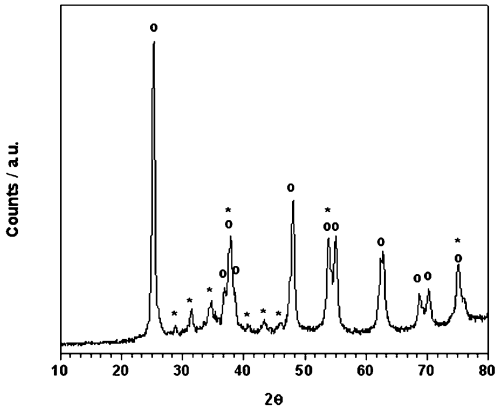

Figure 2. Powder XRD patterns for Ag_2S/TiO_2 nanocomposites (o: anatase; *: acanthite).

Although a SEMSI contribution in the systems reported here is an open issue, we interpret the optical spectra in Figure 3 (part a) as caused by the presence of quantum-sized Ag_2S that for increasing reaction times grows into larger particles. Also note the decrease of reflectance in the visible region with increasing reaction times, which confirms the growth of the metal–sulfide nanophase since less surface area of TiO_2 is available for reflectance of visible light. Part b of Figure 3 shows the absorption spectra for the optically clear supernatant solutions, for the same reaction times, showing no spectral features that could be assigned to Ag_2S nanoparticles, as will be discussed later.

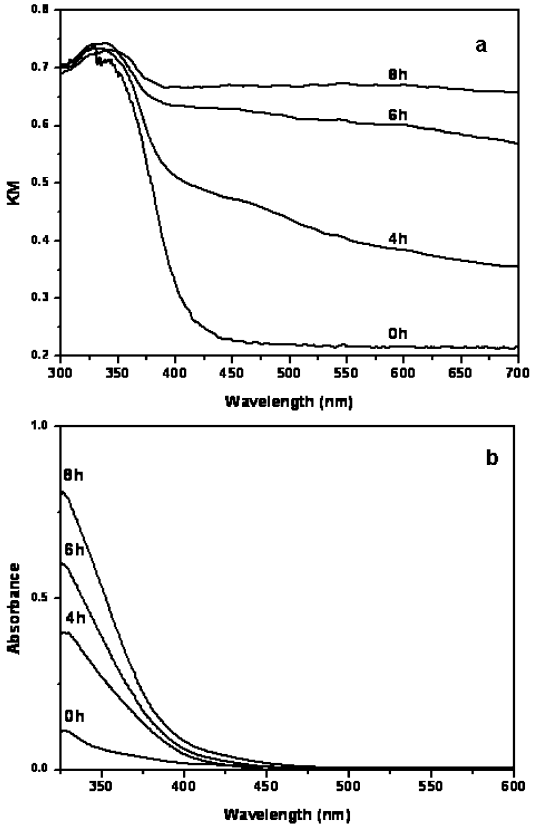

Figure 3. Optical spectra of samples collected at distinct reaction times: a) Kubelka–Munk spectra of the TiO_2/Ag_2S solid nanocomposites; b) absorbance spectra of the supernatant solutions.

For the nanocomposites reported here, the semiconducting nanosized islands tended to grow and coat the TiO_2 surfaces with increasing reaction times. This type of island-like morphology was observed for other substrates besides TiO_2; notably, for amorphous SiO_2 particles used as the substrate, Ag_2S was clearly observed as nanoparticles uniformly distributed over the SiO_2 surfaces, as illustrated in Figure 4. Whereas well-defined and discrete Ag_2S islands were formed at a silica surface, a small number of dispersed Ag_2S islands appeared over the TiO_2 surfaces (Figure 4). Although the focus here is on the synthesis of metal sulfides using TiO_2 substrates, a comparison between the TEM images for Ag_2S grown on SiO_2 and TiO_2 (Figure 4) is valuable because it reveals that the nature of the substrate had a strong effect on the morphology of the final nanostructure. The TiO_2 (anatase) submicron particles provides crystalline surfaces at which selective nucleation of Ag_2S probably occurs. Thereby there is a difference compared with the SiO_2 substrates which are amorphous and at which Ag_2S nanophases have grown randomly at the surface. In both cases, the Ag_2S nano-islands are in fact attached to the substrates as revealed by the magnified TEM images (Figure 4).

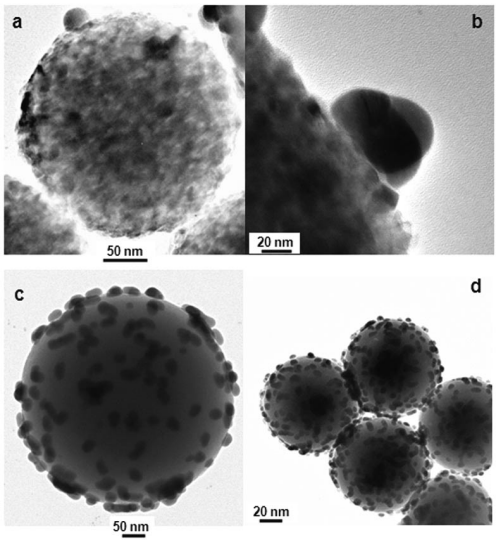

Figure 4. TEM images of nanosized islands of Ag_2S at the surfaces of TiO_2 particles (a and b) and at the surfaces of amorphous SiO_2 particles (c and d).

A possible explanation for the morphology observed in these nanocomposites is that the decomposition of the metal alkyldithiocarbamate into the respective metal sulfide is a surface-mediated reaction, with small metal–sulfide clusters nucleating at the substrates' surfaces. The formation of the metal sulfide proceeds by a controlled release of ionic species coming from the degradation of the single-molecule precursor. This mechanism is also in agreement with earlier observations of the growth of quantum-sized semiconductors at the surface of SiO_2 particles, in which for increasing reaction times the semiconductor bandgap shifted to lower energies.[9]

Yet another possibility is to assume a homogeneous nucleation of metal–sulfide clusters in bulk solution and then their adsorption at the substrates' surfaces. Although we can not rule out this hypothesis, segregated Ag_2S nanophases were not detected by SEM or TEM for the powders collected at the earlier times of reaction. Obviously, such small Ag_2S particles could still remain in solution, but in that case we would also expect optical spectra characteristic of nanodispersed Ag_2S particles, that is, showing an increasing absorption extending to the red region of the spectrum.[13] The spectra of supernatant solutions collected for distinct reaction times show a main band peaked at 300 nm (Figure 3, b), whose intensity increases with reaction time but there is no evidence for an absorption tail at longer wavelengths (500–600 nm). This band in the UV is probably due to molecular species resulting from the precursor decomposition. Finally we note that in the absence of TiO_2

(or SiO_2), the semiconducting phase grows onto the glass walls of the reaction flask where it becomes strongly attached, which together with the earlier results is also experimental evidence for a surface-mediated process.

Thus we propose that the degradation of the single-molecule precursor originates metal–sulfide clusters at the TiO_2 (or SiO_2) surfaces that then coalesce into larger nano islands. As the reaction time increases, the semiconductor phase tends to grow and to mimic the optical properties of the corresponding bulk material. At the moment we can not give a definite explanation for the type of interaction occurring between the metal sulfide and the substrates. The growth of the metal sulfide at the substrate surface is driven by the lattice enthalpy of the solid. On the other hand, the adsorption of precursor species at the surface tends to arrest particle growth, which in this case should have a distinct contribution depending on the substrate used. This possibility is consistent with XPS measurements performed on the SiO_2/Ag_2S and TiO_2/Ag_2S nanocomposites. Whereas for the former we could only assign the Ag3d3 and Ag3d5 peaks to the Ag_2S phase, the XPS of TiO_2/Ag_2S showed two unresolved peaks. These two additional XPS peaks can be related to Ag sites bound to the TiO_2 surface, probably through an oxide bridge (Ag–O–Ti), and thus also confirming the attachment of Ag_2S nanocrystals at the TiO_2 surfaces as suggested by the TEM results.

This discussion requires a chemical step in which sulfide anions are generated and which then react with metal-amine complexes. In order to suggest a chemical mechanism for this process, attempts were made to isolate and characterize intermediate species in reaction mixtures of several metal–alkyldithiocarbamato complexes. This study was limited by the fast kinetics of the reaction decomposition of these complexes into the metal sulfide. Fortunately for one of the compounds investigated, the zinc(II) compound $[Zn(S_2CNEt_2)_2]$, we were able to isolate a powder immediately after the mixture of the starting reagents. This intermediate precursor was identified by elemental analysis as the coordination compound (**I**) $[Zn(H_2NCH_2CH_2NH_2)_3][S_2CN(C_2H_5)]_2$ (calcd. C 35.44, H 8.18, N 20.66; found C 35.08, H 8.27, N 20.38). Unequivocal confirmation for the presence of this intermediate was obtained by comparing the experimental and simulated powder XRD patterns (see Supporting Information) for **I**, whose structural characterization can be found elsewhere.[10]

To confirm this explanation, we performed a NMR spectroscopic study of CD_3OD solutions of **I**, for several reaction times, in the presence of ethylenediamine. In order to obtain accurate NMR spectra, this spectroscopic study was carried out in reaction solutions without TiO_2 (or SiO_2) particles. Figure 5 shows the ^1H NMR peaks of solutions of **I** for distinct reaction times (up to 24 hours). The ^1H NMR spectrum of the starting solution (t = 0 minutes) shows the peaks expected for compound **I**; hence the singlet observed at δ = 2.80 ppm is assigned to the ethylenediamine protons (H^c), and the methylene (H^b) and methyl (H^a) protons from the *N*,*N*-diethyldithiocarbamate anion are assigned at δ = 1.30 ppm (triplet) and 3.90 ppm (quartet), respectively. The protons H^d from ethylenediamine are not observed because they exchange rapidly with the solvent (CD_3OD). We note that during this reaction, the relative intensities of the peaks from the *N*,*N*-diethyldithiocarbamate anion decrease and after one hour they are no longer observed, in agreement with the total decomposition of compound **I**. Meanwhile a number of new peaks appear, which for the earlier times of reaction probably result from a complex mixture of chemical species. However, considering the spectrum recorded for a reaction time of 24 hours, the most intense peak is a singlet observed at δ = 2.80 ppm (H^c), that is, coincident with the peak previously assigned to the ethylenediamine which was in excess in the reaction mixture. Other peaks are a triplet observed at δ = 1.15 ppm, which is probably due to methyl protons (CH_3) of an ethyl group ($H^{b\prime}$), though slightly deviated from the corresponding peaks in the dithiocarbamate anion (δ = 1.30 ppm), and also the methylene protons ($H^{a\prime}$) which appear now deviated at δ = 2.65 ppm relative to the respective protons (H^a, δ = 3.90 ppm) in the initial *N*,*N*-diethyldithiocarbamate anion. On the other hand, a new singlet is observed at δ = 3.67 ppm (H^e), which is about 2/3 of the peak at δ = 1.15 ppm. The protons of these two methylene groups are equivalent because of the prototropy of the 4,5-dihydroimidazole formed in the reaction (Scheme 1).

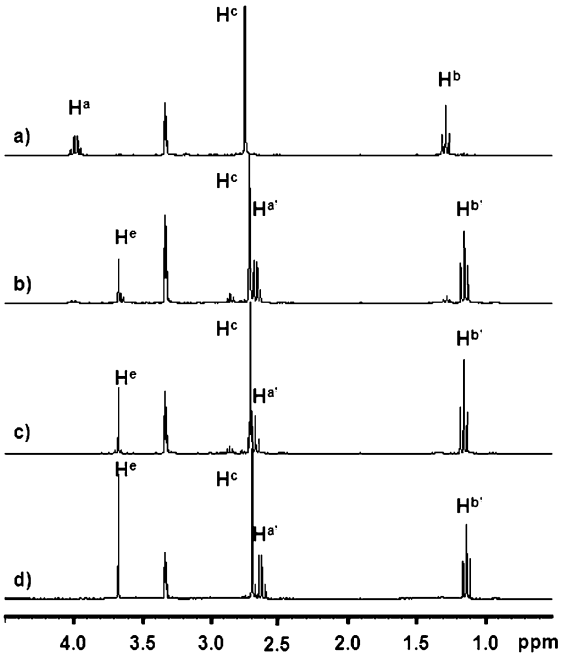

Figure 5. ^1H NMR spectra of refluxed CD_3OD solutions containing $[Zn(S_2CNEt_2)_2]$ and ethylenediamine, for distinct reaction times: a) 0 h; b) 1 h; c) 2 h; d) 24 h.

Scheme 1 shows a possible mechanism which agrees with our spectroscopic data; the ^1H NMR spectrum at the bottom assigns the peaks to the respective protons labelled in Scheme 1 for the organic compound obtained at the end of the reaction. Thus the *N*,*N*-diethyldithiocarbamate anion reacts in the presence of ethylenediamine forming in the end the cyclic compound, 2-diethylamino-4,5-dihydro-1*H*-

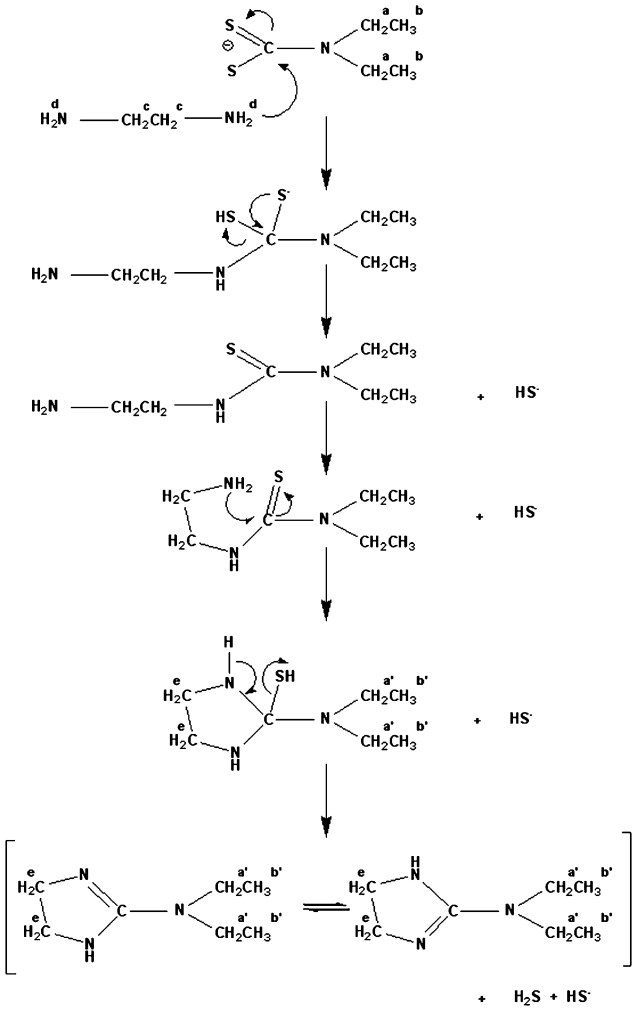

Scheme 1. Mechanism for the generation of sulfide ions from *N*-alkyldithiocarbamates in the presence of ethylenediamine (CD_3OD solutions).

imidazole, and hydrogen sulfide. The latter readily ionizes to generate the metal sulfide according to the overall equilibrium:

$$[Zn(en)_3]^{2+} + S^{2-} \longrightarrow ZnS + 3\,en$$

More convincing evidence for this mechanism comes from examining the ^{13}C NMR spectra of the initial (t = 0 hours) and final (t = 24 hours) reaction mixtures. In terms of this mechanism, one should expect four distinct peaks: four peaks from 2-diethylamino-4,5-dihydro-1*H*-imidazole and one from the ethylenediamine in excess in the reaction mixture, and indeed all these peaks were observed at δ = 14.7, 44.5, 45.0, 45.7 and 165.5 ppm (see Supporting Information). The peak at δ = 165.5 ppm appears as a broad and low intensity signal due to the previously mentioned prototropy of the *S*-substituted imidazole ring (Scheme 1).[14] In addition the characteristic peak of CS_2, observed at δ = 205.9 ppm in the spectrum of the original precursor, was no longer observed in the final solution.

This discussion shows that in the growing process, the *N*-alkyldithiocarbamate anion acts as a sulfide source: this anion being generated in situ in a controlled process. On the other hand, the metal complexes are probably adsorbed at silica surfaces that tend to favour dissociation of the organic ligands from the metal centre, hence favouring the formation of the metal sulfide in equilibrium 1. As a result, morphological well-defined nanoparticles can be prepared by adjusting the synthetic conditions favouring the controlled release of cations (equilibrium 1) and the controlled generation of sulfide ions (Scheme 1). This opens up the possibility of a selective choice of the amines used to control the growth of the metal–sulfide nanophases.

An important feature of the TiO_2-based nanocomposites prepared by the method reported here is that the nanophases are evenly dispersed as islands and do not completely cover the TiO_2 surface. The Ag_2S/TiO_2 nanocomposites are particularly interesting because the Ag_2S islands are arrested at the TiO_2 surfaces but are still chemically reactive, and therefore they could be partially reduced to metal silver, yielding Ag-supported TiO_2 materials with potential interest in photocatalysis, as schematically illustrated in Figure 6.[15]

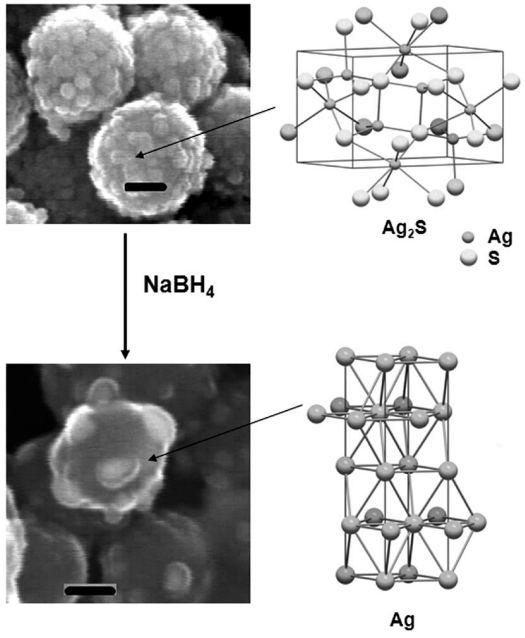

Figure 6. Chemical and morphological transformation of nano-islands of Ag_2S into Ag, at the TiO_2 nanoparticles surface, in the presence of aqueous $NaBH_4$ (bar length corresponds to 100 nm).

Conclusions

In summary, coupled Ag_2S/TiO_2 nanocomposites were prepared from a heterogeneous reaction system containing metal *N*-alkyldithiocarbamates as the precursors and TiO_2 submicron particles as the substrates, in acetone medium. A possible mechanism for the formation of the metal–sulfide nanophases through this one-step reaction was presented on the basis of microscopic characterization of the solid phases and NMR spectroscopic analysis of the reaction

solutions. This mechanism successfully explains the growth of metal sulfides, by applying a controlled release of anions from the precursor to the reaction solution. In addition, this synthetic method opens up the possibility of chemical design of coupled nanocomposites for several photo-applications,[16,17] since a variety of materials can be tailored by varying the deposited phase and the type of substrate, both in terms of shape and chemical composition.

Experimental Section

General: All chemicals were supplied by Aldrich, except ethanol (Riedel-de Haën), and were used as received.

The Ag^I dithiocarbamato complex was prepared by the stoichiometric reaction of $Na[S_2CN(CH_2CH_3)_2]$ and the respective metal nitrate, in water. The solids obtained were isolated by filtration and washed with distilled water. The purity of the metal complexes was checked by IR and ^1H NMR spectroscopy.

Silica particles were prepared using the Stöber method:[18] Tetraethoxysilane (TEOS, 0.73 g) was added to absolute ethanol (5 mL) containing distilled water (0.06 g), and the mixture was allowed to stand for 30 min. Subsequently, 25% NH_4OH solution (2 mL) was added to the reaction mixture, and the solution left to stand for 30 min. The colloid formed was filtered and washed thoroughly with water and ethanol. The SiO_2 particles were then used after a thermal treatment at 700 °C for 4 h.

Spherical TiO_2 (anatase) particles were prepared by the controlled hydrolysis of titanium tetraethoxide in ethanol as described by Maret.[19] Using this method the particle size can be varied by adjusting the relative amounts of $Ti(OEt_4)_4$ and water, or by varying the type of metal–alkali salt added to the reaction mixture. In a typical synthesis, ethanol (100 mL) was mixed with 0.1 M aqueous solution of KCl (0.4 mL), followed by addition of $Ti(OC_2H_5)_4$ (1.7 mL), at room temp. and under magnetic stirring. The reaction ran over 8 h, yielding in the end a colourless colloid. The solid was then collected on a millipore membrane (0.25 μm), forming a compact coating, and this amorphous TiO_2 was thoroughly washed with ethanol/water. The crystalline phase anatase-TiO_2 was obtained by placing the solid in alumina crucibles, followed by thermal treatment at 500 °C for 4 h in a tubular oven.

All the nanocomposite particles were prepared by adding ethylenediamine (2.5 mL) dropwise to an acetone solution (25 mL) containing the Ag^I dithiocarbamato complex (0.125 mmol) and TiO_2 (or SiO_2) particles (0.125 g). The suspension formed was then refluxed with stirring under a N_2 stream. Samples were collected for distinct reaction times, and the solids were isolated by centrifugation and washed thoroughly with acetone. All the powders were prepared and collected inside a well-ventilated fume-cupboard and were then dried at room temp. in a desiccator under vacuum.

The absorption spectra were recorded with a Jasco V-560 UV/Vis spectrophotometer. Transmission electron microscopy (TEM) was carried out with a JEOL 200CX microscope operating at 300 kV. The samples were prepared as follows: an aliquot containing the nanocomposite dispersed in acetone was placed on a copper grid coated with an amorphous carbon film and the solvent was then evaporated. Scanning electron microscopy (SEM) and energy-dispersive X-ray spectroscopy (EDX) were performed using a FEG-SEM Hitachi S4100 microscope operating at 25 kV. The samples were prepared by deposition of an aliquot of the suspension of the nanocomposite in acetone on aluminium pieces and then coated with evaporated carbon.

The NMR spectroscopic experiments were conducted with a Bruker Advance 300 NMR spectrometer using CD_3OD (Aldrich) as the solvent. To monitor the reaction over time, the compound $[Zn(H_2NCH_2CH_2NH_2)_3][S_2CN(C_2H_5)]_2$ (0.157 mmol, 0.085 g) and ethylenediamine (0.24 mmol, 20 μL) were placed in CD_3OD (15 mL), and this mixture was then refluxed under magnetic stirring and a N_2 flow. For the required reaction times, samples (2 mL) of the reaction solution were collected and centrifuged, to remove any solid particulates formed, and then analysed by NMR spectroscopy.

X-ray photoelectron spectroscopy (XPS) was performed in the CAE mode (30 eV) using a Microlab 370 F instrument with an Al (non-monochromatic) anode. The accelerating voltage was 15 kV. The quantitative XPS analysis was performed using the Avantage software.

Supporting Information (see also the footnote on the first page of this article): (a) ^{13}C NMR spectra of CD_3OD solutions containing $[Zn(S_2CNEt_2)_2]$ and ethylenediamine; (b) experimental and simulated powder XRD patterns of the intermediate zinc(II) compound; (c) selected XPS peaks of the nanocomposites.

Acknowledgments

M. C. N. thanks the University of Aveiro for a PhD grant, and O. C. M. thanks FCT for the grant SFRH/BPD/14554/2003. This work was supported by FCT/FEDER with funding through the project POCI/QUI/5961/2004.

[1] a) G. A. Ozin, A. C. Arsenault, *Nanochemistry*, RSC, Cambridge, **2005**; b) G. Schmid (Ed.), *Nanoparticles*, Wiley-VCH, Weinheim, **2004**; c) C. N. R. Rao, A. Müller, A. K. Cheetham (Eds.), *The Chemistry of Nanomaterials*, Wiley-VCH, Weinheim, **2003**.

[2] a) P. V. Kamat, *Chem. Rev.* **1993**, *93*, 267–300; b) A. Mills, R. H. Davies, D. Worsley, *Chem. Soc. Rev.* **1993**, *22*, 417–425; c) D. Bahnemann, *Solar Energy* **2004**, *77*, 445–459.

[3] D. Beydoun, R. Amal, G. Low, S. McEvoy, *J. Nanoparticle Res.* **1999**, *1*, 439–458.

[4] a) P. Mulvaney, L. M. Liz-Marzán, M. Giersig, T. Ung, *J. Mater. Chem.* **2000**, *10*, 1259–1269; b) M. A. Malik, P. O'Brien, N. Revaprasadu, *Chem. Mater.* **2002**, *14*, 2004–2010; c) M. C. Neves, L. M. Liz-Marzán, T. Trindade, *J. Colloid Interface Sci.* **2003**, *264*, 391–395; d) K. D. Kim, H. J. Bae, H. T. Kim, *Colloids. Surf. A* **2003**, *224*, 119–126; e) T. Tago, Y. Shibata, T. Hatsuta, K. Miyajima, M. Kishida, S. Tashiro, K. Wakabayashi, *J. Mater. Sci.* **2002**, *37*, 977–982; f) Y. Chan, J. P. Zimmer, M. Stroh, J. S. Steckel, R. K. Jain, M. G. Bawendi, *Adv. Mater.* **2004**, *16*, 2092–2097.

[5] a) O. Dabbousi, J. Rodriguez-Viejo, F. V. Mikulec, J. R. Heine, H. Mattoussi, R. Ober, K. F. Jensen, M. G. Bawendi, *J. Phys. Chem. B* **1997**, *101*, 9463–9475; b) D. V. Talapin, I. Mekis, S. Goltzinger, A. Kornowski, O. Benson, H. Weller, *J. Phys. Chem. B* **2004**, *108*, 18826–18831; c) A. Sashchiuk, L. Langof, R. Chaim, E. Lifshitz, *J. Cryst. Growth* **2002**, *240*, 431–438.

[6] a) R. Vogel, P. Hoyer, H. Weller, *J. Phys. Chem.* **1994**, *98*, 3183–3188; b) S. Somasundaram, C. R. Chenthamarakshan, N. R. Tacconi, Y. Ming, K. Rajeshwar, *Chem. Mater.* **2004**, *16*, 3846–3852; c) D. Shchukin, S. Poznyak, A. Kulak, P. Pichat, *J. Photochem. Photobiol. A: Chem.* **2004**, *162*, 423–430; d) A. Kitiyanan, T. Kato, Y. Suzuki, S. Yoshikawa, *J. Photochem. Photobiol. A: Chem.* **2006**, *179*, 130–134.

[7] a) D. C. Bradley, *Chem. Rev.* **1989**, *89*, 1317–1322; b) P. O'Brien, R. Nomura, *J. Mater. Chem.* **1995**, *5*, 1761–1773; c)

M. Bochmann, *Chem. Vap. Deposition* **1996**, *2*, 88–96; d) O. C. Monteiro, T. Trindade, F. A. Almeida Paz, J. Klinowski, J. Waters, P. O'Brien, *J. Mater. Chem.* **2003**, *13*, 3006–3010; e) M. Afzaal, K. Ellwood, N. L. Pickett, P. O'Brien, J. Raftery, J. Waters, *J. Mater. Chem.* **2004**, *14*, 1310–1315.

[8] a) T. Trindade, P. O'Brien, *Adv. Mater.* **1996**, *8*, 161–163; b) S. L. Cumberland, K. M. Hanif, A. Javier, G. A. Khitrov, G. F. Strouse, S. M. Woessner, C. S. Yun, *Chem. Mater.* **2002**, *14*, 1576–1584; c) T. G. Schaaff, A. J. Rodinone, *J. Phys. Chem. B* **2003**, *107*, 10416–10422; d) M. Green, P. Prince, M. Gardener, J. Steed, *Adv. Mater.* **2004**, *16*, 994–996; e) M. D. Regulacio, N. Tomson, S. L. Stoll, *Chem. Mater.* **2005**, *17*, 3114–3121; f) Y. Wada, M. Kaneko, D. Niinobe, Y. Tsukahara, *Chem. Lett.* **2005**, *34*, 1618–1619.

[9] a) O. C. Monteiro, A. C. C. Esteves, T. Trindade, *Chem. Mater.* **2002**, *14*, 2900–2904; b) O. C. Monteiro, M. C. Neves, T. Trindade, *J. Nanoscienc. Nanotechnology* **2004**, *4*, 137–141; c) M. C. Neves, J. Soares, R. Hempelmann, T. Monteiro, T. Trindade, *J. Cryst. Growth* **2005**, *279*, 433–438.

[10] a) L. Glinskaya, S. Zemskova, R. Klevtsova, S. Larionov, S. Gromilov, *Polyhedron* **1992**, *11*, 2951–2956; b) L. A. Glinskaya, S. M. Zemskova, R. F. Klevtsova, *Zh. Strukt. Khim. (Russ.) (J. Struct. Chem.)* **1998**, *39*, 353.

[11] J. P. Espinós, A. I. Martín-Concepción, C. Mansilla, F. Yubero, A. R. González-Elipe, *J. Vac. Sci. Technol. A* **2006**, *24*, 919–928.

[12] a) H. Weiss, A. Fernandez, H. Kisch, *Angew. Chem. Int. Ed.* **2001**, *40*, 3825–3827; b) H. Kisch, H. Weiss, *Adv. Funct. Mater.* **2002**, *12*, 483–488; c) M. Gartner, V. Dremov, P. Müller, H. Kisch, *ChemPhysChem* **2005**, *6*, 714–718.

[13] a) P. Hoyer, H. Weller, *Chem. Phys. Lett.* **1994**, *224*, 75–80; b) L. Motte, F. Billoudet, M. P. Pilleni, *J. Phys. Chem.* **1995**, *99*, 16425–16429; c) A. I. Kryukov, A. L. Stroyuk, N. N. Zinchuk, A. V. Korzhak, S. Ya. Kuchmii, *J. Mol. Catal. A* **2004**, *221*, 209–221; d) A. N. Rodriguez, M. T. S. Nair, P. K. Nair, *Semicond. Sci. Technol.* **2005**, *20*, 576–585.

[14] J. Mäki, R. Sjöholm, L. Kronberg, *J. Chem. Soc. Perkin Trans. 1* **2000**, *1*, 4445–4450.

[15] a) P. V. Kamat, *J. Phys. Chem. B* **2002**, *106*, 7729–7744; b) D. Shchukin, E. Ustinovich, D. Sviridov, P. Pichat, *Photochem. Photobiol. Sci.* **2004**, *3*, 142–144; c) P. D. Cozzoli, M. L. Curri, C. Giannini, A. Agostiano, *Small* **2006**, *2*, 413–421.

[16] a) A. Fujishima, T. N. Rao, D. A. Tryk, *J. Photochem. Photobiol. C: Photochem. Rev.* **2000**, *1*, 1–21; b) K. Ramalingam, G. Aravamudan, V. Venkatachalam, *Bull. Chem. Soc. Jpn.* **1993**, *66*, 1554–1555; c) S. Lo, C. Lin, C. Wu, P. Hsieh, *J. Hazard. Mater.* **2004**, *B114*, 183–190; d) M. G. Kang, H. E. Han, K. J. Kim, *J. Photochem. Photobiol. A: Chem.* **1999**, *125*, 119–125; e) H. Fujii, M. Ohtaki, K. Eguchi, H. Arai, *J. Mol. Catal. A* **1998**, *129*, 61–68; f) J. M. Stipkala, F. N. Castellano, T. A. Heimer, C. A. Kelly, K. J. T. Livi, G. J. Meyer, *Chem. Mater.* **1997**, *9*, 2341–2353.

[17] M. Grätzell, *Pure Appl. Chem.* **2001**, *73*, 459–467.

[18] W. Stöber, A. Fink, E. Bohn, *J. Colloid. Interf. Sci.* **1968**, *26*, 62–69.

[19] S. Eiden-Assmann, J. Widoniak, G. Maret, *Chem. Mater.* **2004**, *16*, 6–11.

Received: January 29, 2008
Published Online: August 28, 2008

